Detection of High-Affinity Intercalator Sites in a Ribosomal RNA Fragment by the Affinity Cleavage Intercalator Methidiumpropyl-EDTA–Iron(II)†

Joanne M. Kean, Susan A. White, and David E. Draper*
Department of Chemistry, Johns Hopkins University, Baltimore, Maryland 21218
Received October 2, 1984

ABSTRACT: The affinity cleavage reagent methidiumpropyl-EDTA (MPE) [Hertzberg, R. P., & Dervan, P. B. (1982) *J. Am. Chem. Soc. 104*, 313–315] intercalates between base pairs in helical DNA and, when complexed with Fe(II), cleaves the DNA by oxidative degradation of the deoxyribose. We find that this reagent is useful for mapping structure in some RNA molecules. The reagent binds to poly(A)-poly(U) with the same or slightly lower affinity as the related ethidium intercalator, selectively binds double-helical in preference to single-stranded RNA, and when complexed with Fe(II) readily cleaves the RNA backbone. The reagent binds to three or four helical locations in $tRNA^{Phe}$ with an affinity of 10^5–10^6 M^{-1} (0.1 M Na^+, pH 7.6, 37 °C). With a 345-base RNA fragment covering the S8/S15 protein binding region of *Escherichia coli* 16S ribosomal RNA, MPE–Fe(II) intercalates strongly at two helical sites: one is located at or near a single base bulge and the other at the end of a helix. Intense cutting is also seen in a region that is not part of a Watson–Crick helix. Ethidium bromide binds at these sites with high affinity (about 10^7 M^{-1} at 0.1 M Na^+, pH 7.6, 37 °C). The sites are all clustered in a region of the RNA thought to bind S15. Tertiary folding of the RNA may distort helices in the molecule to create sites with particularly high affinities for intercalators; such sites may have functional significance in protein recognition or RNA–RNA interactions.

Structure mapping is a useful tool for investigating RNA folding. In this approach, an RNA specie is end labeled with ^{32}P and cleaved by a reagent with specificity for particular RNA conformations, and the cleavage sites are determined by high-resolution gel electrophoresis of the fragments (Wurst et al., 1978). The first structure-specific reagents used were enzymes with single strand specificity such as S_1 nuclease (Wurst et al., 1978). An enzyme specific for double-helical RNA, cobra venom V_1 nuclease, has been purified and used to obtain complementary information (Lockard & Kumar, 1981; Auron et al., 1982). The chemical reagents dimethyl sulfate and diethyl pyrocarbonate have been used as probes for unstructured RNA (Peattie & Gilbert, 1980). With this array of reagents the major secondary features of an RNA molecule can generally be deduced [e.g., 5S RNA (Garrett & Oleson, 1983), 3′ terminus of 16S rRNA (Douthewaite et al., 1983), and the S8/S15 binding region of 16S rRNA (Kean & Draper, 1985)].

The detail attainable by structure mapping is currently limited by the specificity of the probes available. In tRNA, and presumably most other RNAs, most bases are hydrogen bonded and stacked in specific structures (Holbrook et al., 1978), yet only one available probe, cobra venom nuclease V_1, has specificity for structured (in this case, double-helical) RNA. We find the properties of the affinity cleaving reagent methidiumpropyl-EDTA (MPE)[1] promising as another "structure-specific" reagent. MPE is a methidium intercalator moiety tethered to EDTA; upon addition of Fe(II) and a reducing agent the ferrous ion binds the EDTA and generates short-lived radicals that cleave nearby polynucleotide backbones (Hertzberg & Dervan, 1982, 1984). The high preference of the closely related ethidium intercalator for double-helical over single-stranded polynucleotides is well established (LePecq & Paoletti, 1967). To see if MPE is useful as a structure-specific reagent, we have mapped its cutting sites in $tRNA^{Phe}$ and a 345-base fragment of 16S rRNA (Kean & Draper, 1985) and determined its affinity for various RNA sites. Our results show that MPE cutting patterns can give useful clues to RNA folding, particularly when combined with estimations of MPE affinity for particular sites.

Materials and Methods

Chemicals. All solutions were made up with water purified through a Millipore "Milli-Q" apparatus. MPE was a generous gift from Peter Dervan. Yeast $tRNA^{Phe}$ was purchased from Sigma, ethidium bromide was from CalBiochem, ammonium iron(II) sulfate was from Aldrich, polynucleotides were from Pharmacia and P-L Biochemicals, RNA ligase, T_1 ribonuclease, and polyacrylamide gel reagents were from BRL, and ^{32}P nucleotides were from Amersham.

Labeled RNAs. $tRNA^{Phe}$ was 3′ end labeled with RNA ligase and cytidine 3′,5′-[^{32}P]bisphosphate under the conditions described by D'Alessio (1982). The reaction mix was run on a 40- or 85-cm sequencing gel and the full-length tRNA band located by autoradiography and cut out. RNA was extracted from the gel and phenol extracted as described previously (Kean & Draper, 1985). The tRNA was stored in 0.2 M NaCl and 50 mM Tris, pH 7.6, at −70 °C, and renatured for 5 min at 65 °C before use.

F61 RNA is a 345-base fragment from the *Escherichia coli* 16S ribosomal RNA, covering bases 525–869 in the sequence (Noller & Woese, 1981). It was made by a hybridization selection method; its preparation and 5′ and 3′ end labeling are described in detail in the preceding paper (Kean & Draper, 1985).

MPE–Fe(II) Reactions. The standard MPE–Fe(II) cleavage reaction contained 25 mM Tris, pH 7.6, 0.1 M NaCl, 1 μM each of MPE and ammonium iron(II) sulfate, and 2

† This research was supported by National Institutes of Health Grant GM-29048 and by Grant BRSG SO7 RR7041 awarded by the Biomedical Research Support Program, Division of Research Resources, National Institutes of Health.

[1] Abbreviations: MPE, methidiumpropyl-EDTA; EDTA, ethylenediaminetetraacetic acid; Tris, tris(hydroxymethyl)aminomethane; DTT, dithiothreitol.

0006-2960/85/0424-5062$01.50/0

mM DTT. Reactions performed at different concentrations of MPE always contained equal concentrations of Fe(II). Ammonium iron(II) sulfate was dissolved in water immediately before use and quickly diluted with MPE to form a stock solution 0.2 mM in MPE–Fe(II). Dilutions of this stock were made, if necessary, and added to the RNA solution, immediately followed by the DTT. The standard incubation was at 37 °C for 20 min; at the end of this time the reaction was diluted with an equal volume of 10 M urea containing gel tracking dyes, placed on ice, and immediately loaded on a sequencing gel. Gels were standard 50% urea and 8%, 12%, or 20% polyacrylamide in TBE buffer (D'Alessio, 1982), poured in a 0.04 × 18 × 85 cm mold, and run at 30–40 W constant power.

Fluorescence Titrations. Fluorescence titrations were performed in a Perkin-Elmer MPF44B fluorometer. The cell holder was thermostated by a circulating water bath. Titrations with ethidium bromide were in a volume of 3.0 mL in a 1 cm × 1 cm cuvette; MPE titrations were in 0.6 mL in a 4 mm × 4 mm cuvette or 0.8 mL in a 5 mm × 10 mm cuvette. MPE was excited at 469 nm, and emission was monitored at 645 nm; for ethidium the wavelengths were 494 and 590 nm, respectively.

To calculate a binding affinity, several initial concentrations of intercalator (ethidium bromide or MPE) were titrated with polynucleotide. At sufficiently high intercalator concentrations added polynucleotides are saturated with intercalator until all the intercalator is consumed; the break point of such a titration gives the number of base pairs per intercalator at saturation (i.e., the reciprocal of the site size). These site sizes varied between 2.6 and 3.0 base pairs per intercalator. Titrations at lower intercalator concentrations were then fit to the McGhee & von Hippel (1974) equation which takes into account the potential "overlap" of ligand sites on polynucleotides:

$$v = KL(1 - nv)\left(\frac{1 - nv}{1 - (n - 1)v}\right)^{n-1}$$

Where K is the equilibrium constant, n the site size, L the free ligand concentration, and v the saturation (intercalators per base pair). If the data were not fit well by using this isotherm, then cooperativity was introduced into the above equation [detailed in McGhee & von Hippel (1974)] and different pairs of K and w (the cooperativity parameter) were examined. The equilibrium constants reported are each averaged from two to five titrations at different intercalator concentrations.

Calculation of MPE–Fe(II) Affinity Constants from Competition Experiments. If the extent of MPE–Fe(II) cleavage at a site is proportional to the degree of saturation at that site, then it is possible to derive the MPE–Fe(II) affinity at the site by observing the cutting intensity as a function of free MPE–Fe(II) concentration. Reproducible results were obtained by buffering MPE–Fe(II) to very low free concentrations with poly(A)-poly(U); i.e., the free concentration of MPE–Fe(II) is given by $[\text{MPE–Fe(II)}]_f = [\text{MPE–Fe(II)}]_0/(1 + K[\text{poly(A)-poly(U)}]_0)$ if $[\text{poly(A)-poly(U)}]_0 \gg [\text{MPE–Fe(II)}]_0$ (zero subscripts refer to total concentrations). The concentration of tRNA or F61 RNA was always very small compared to the total MPE–Fe(II) concentration and thus did not affect the buffering of free MPE–Fe(II). The intensity of cutting at a particular site, I, and the free MPE–Fe(II) concentration were plotted in the double-reciprocal format, $1/I = 1/(I_0K[\text{MPE–Fe(II)}]_f) + 1/I_0$, to obtain the affinity constant K and the maximum cutting intensity I_0 from the slope and intercept.

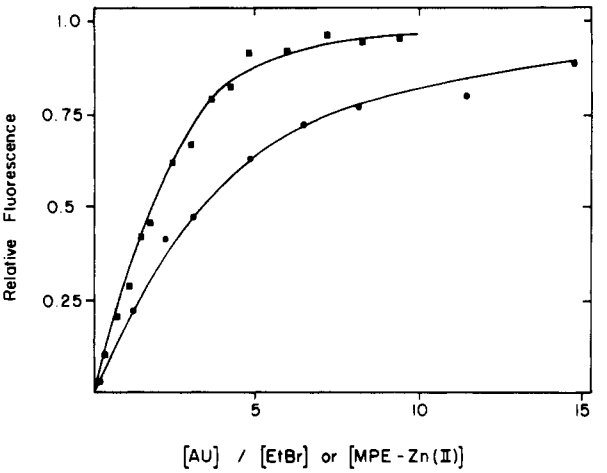

FIGURE 1: Fluorescence titration of ethidium bromide or MPE–Zn(II) with poly(A)-poly(U). Titrations are at 37 °C in 20 mM Tris, pH 7.6, and 100 mM NaCl. (■) 2.8 μM ethidium bromide. Curve is an overlap binding isotherm calculated with $K = 0.6 \times 10^6$ M^{-1}, $n = 3$ bases, and $w = 5$. The extrapolated maximum fluorescence enhancement is 11.3-fold. (●) 5.07 μM MPE–Zn(II). The curve is calculated with $K = 0.16 \times 10^6$ M^{-1}, $n = 3$ bases, and $w = 1$. The extrapolated maximum fluorescence enhancement is 2.55-fold.

Table I: Affinities of Ethidium Bromide, MPE–Zn(II), and MPE–Fe(II) for Poly(A)-Poly(U) Determined by Fluorescence Titration

intercalator	[NaCl] (mM)[a]	T (°C)	K (μM^{-1})[b]	w
EthBr	50	23	1.0 ± 0.2	3
EthBr	100	37	0.6 ± 0.2	5
MPE–Zn(II)	50	23	0.6 ± 0.2	1
MPE–Zn(II)	100	23	0.35 ± 0.2	1
MPE–Zn(II)	200	23	0.13 ± 0.05	1
MPE–Zn(II)	100	37	0.16 ± 0.05	1
MPE–Fe(II)	50	23	0.6 ± 0.3	1

[a] Standard titration conditions were 20 mM Tris, pH 7.6, 20 °C, and the indicated salt concentration. [b] Equilibrium binding constant (K) and site size (n) calculated as described under Materials and Methods; site sizes ranged between 2.6 and 3 for all determinations.

All X-ray films were preflashed to ensure a linear relation between film density and quantity of ^{32}P (Laskey, 1982). Films were scanned on a Joyce-Loebl Chromoscan 3 densitometer using a 0.25 × 5 mm beam.

RESULTS

Comparison of MPE and Ethidium Binding to Double-Helical RNA. The affinity of MPE–Zn(II) for the synthetic RNA poly(A)-poly(U) was measured by observing the increase in MPE fluorescence with addition of RNA; identical experiments were done with ethidium bromide. Representative data are shown in Figure 1 and summarized in Table I. The ethidium titration data were fit best by isotherms including modest cooperativity ($w = 3$–5); Bresloff & Crothers (1981) also found some cooperativity in ethidium binding to poly(A)-poly(U). Titrations with MPE–Zn(II) could not be fit with cooperativity in this range and were best accommodated by w between 0.5 and 1. Binding isotherms tend to be more sensitive to the product Kw than to either K or w individually, which contributes some uncertainty to our determinations of intrinsic binding affinities, particularly for ethidium. We estimate that ethidium binds poly(A)-poly(U) with equal or somewhat greater (up to 4-fold) affinity than MPE–Zn(II).

MPE–Zn(II) binding is weakly dependent on the monovalent ion concentration (Table I), and the dependence is roughly equivalent to that of ethidium (LePecq & Paoletti, 1967); i.e., MPE–Zn(II) behaves approximately as an ion of 1+ charge

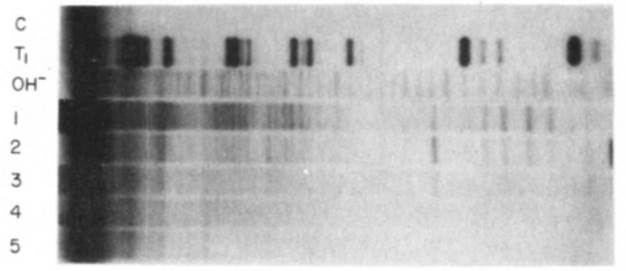

FIGURE 2: Sequencing gel displaying MPE–Fe(II) cutting sites in $tRNA^{Phe}$. The tRNA is 3′ end labeled and reacted as described under Materials and Methods. C, no digestion; T_1, T_1 ribonuclease digestion under denaturing conditions; OH^-, alkaline hydrolysis; 1–5, reaction with 1.3 μM MPE–Fe(II) and 4.93, 13.1, 39.4, 78.8, and 197 μM poly(A)-poly(U) base pairs, respectively.

Table II: Influences of Salts and Competitors on MPE–Fe(II) Cutting of $tRNA^{Phe}$ [a]

[NaCl] (mM)	[$MgCl_2$] (mM)	competitor	relative cutting strength
100	0		1.00
200	0		0.74
100	1		0.42
100	10		0.13
100	0	530 μM poly(A)	0.92
100	0	130 μM poly(A)-poly(U)	0.05

[a] Cutting conditions were 10 μM MPE–Fe(II) and 20 mM Tris, pH 7.6, plus indicated salts, incubated at 37 °C for 20 min. With 100 mM NaCl 28% of the tRNA molecules remained uncut. Relative cutting strength was estimated by integrating the total intensity of cut molecules.

in its electrostatic interactions with RNA (Record et al., 1976). Since MPE–Zn(II) is actually a zwitterion (methidium has a 1+ charge and the EDTA–Zn(II) complex a 1− charge), it appears that the EDTA–Zn(II) complex is not bound close enough to the RNA to significantly perturb the atmosphere of bound counterions. The EDTA–Zn(II) charge could contribute an unfavorable free energy to MPE–Zn(II) binding at adjacent sites on a polymer (i.e., anticooperativity), which may explain the difference in cooperativity observed between ethidium and MPE–Zn(II).

Experiments reported below used RNA cleavages induced by MPE–Fe(II) in the presence of DTT to determine the affinity of MPE–Fe(II) for individual sites in an RNA molecule [a reducing agent is required to obtain significant cleavage by the EDTA–Fe(II) moiety]. To see if MPE–Fe(II)–DTT binds RNA much differently than MPE–Zn(II), we first attempted to determine the affinity of MPE–Fe(II) for poly(A)-poly(U) in the absence of DTT. To minimize damage to the RNA by the presence of Fe(II), these titrations were completed within 30 min; titrations were also checked at different points for time-dependent changes in fluorescence. Substitution of Fe(II) for Zn(II) did not significantly affect the MPE affinity (Table I). Attempts to repeat these titrations with DTT present were not successful, as the fluorescence intensity changed too rapidly with time. We did prepare poly(A)-poly(U) with different degrees of MPE–Fe(II) saturation, then rapidly added DTT to 2 mM, and looked for immediate fluorescence changes that might indicate a significant change in affinity. None was observed. We conclude that our fluorescence measurements of MPE–Zn(II) affinity hold approximately for MPE–Fe(II) in the presence of DTT.

Cleavage of tRNA by MPE–Fe(II). Studies by Hertzberg & Dervan (1982, 1984) indicate that MPE–Fe(II) reacts with O_2 to produce a short-lived, diffusible specie, perhaps hydroxyl radical, which cleaves the DNA backbone by oxidative degradation of the sugar. The reaction releases a free base and leaves (most likely) a 5′-phosphate and a mixture of 3′-phosphate and 3′-phosphoglycolic acid at the cleavage ends. We cleaved both 5′-end-labeled and 3′-end-labeled RNA molecules with MPE–Fe(II) and found the same cleavage pattern displayed on gels as with DNA, i.e., heterogeneous 3′ termini and a homogeneous 5′ terminus retaining a phosphate (data not shown). DNA and RNA cleavage mechanisms thus appear similar. The heterogeneous 3′ termini make the resolution of 5′-end-labeled material on gels poor for all but very short fragments; we therefore used mainly 3′-end-labeled RNA.

An RNA of known structure, yeast $tRNA^{Phe}$, was reacted under standard conditions (0.1 M Na^+, pH 7.6, 37 °C) with free MPE–Fe(II) concentrations ranging from 0.1 to 10 μM and the cleavage products determined on sequencing gels (see Figure 2). Groups of several strong cuts interspersed with regions of relatively weak cutting are seen. Inclusion of 1 mM Mg^{2+} in the reaction did not significantly alter the cutting pattern (data not shown). Several control experiments ensure that the pattern of cuts observed is actually a result of strong MPE binding to the tRNA (Figure 2 and Table II; data not shown). High concentrations of poly(A) (up to 500 μM) in the reaction mixture had little influence on the pattern or total intensity of cuts, while lower concentrations of poly(A)-poly(U) practically eliminated the cleavage intensity. This shows that MPE–Fe(II) does not bind the RNA by a weak, nonspecific mechanism but with an affinity comparable to that of intercalation. A more quantitative estimate of affinities is made below. The EDTA–Fe(II) complex alone at 20 μM gave virtually no cleavage. Occasionally cleavage at single bases, rather than clusters of bases, was seen with MPE–Fe(II) [see Figure 2, particularly the lanes with higher poly(A)-poly(U) concentrations]. These cuts were generally at pyrimidine–purine sequences and were also found when Fe(II) or other transition metals were incubated with the RNA. We presume these single base cuts are due to metal-catalyzed RNA hydrolysis (Britten, 1962; Brown et al., 1983) and not to MPE–Fe(II) binding and cutting.

The relative intensity of MPe–Fe(II) cleavage along the linear tRNA sequence is plotted in Figure 3A, and the major cut sites are indicated in a sketch of the tRNA tertiary structure in Figure 3B. Because the MPE-propyl tether is flexible and the radicals generated are able to diffuse a short distance, the EDTA–Fe(II) complex generates sets of three to five cleavages. A consequence of DNA geometry is that the most intense cleavages on opposite strands of a helix are staggered to the 3′ side of the EDTA–Fe(II) moiety (Schultz et al., 1982; Schultz & Dervan, 1983). Models built with the A-form geometry of RNA suggest that the same staggering of cuts should hold with MPE–Fe(II) intercalated at specific sites in an RNA double helix. The cuts in the anticodon stem show this alignment and indicate MPE–Fe(II) intercalation between base pairs C27-G43 and C28-G42. The positions of MPE–Fe(II) binding sites which generate the other observed cuts are dealt with under Discussion.

Influence of Salts on MPE–Fe(II) Cleavage. Table II summarizes the effects of Na^+ and Mg(II) ions on MPE–Fe(II) cleavage of tRNA. There is a weak effect of Na^+ on cutting, as expected from the salt dependence of MPE–Zn(II) binding (Table I). Mg(II) has a much greater effect: 10 mM virtually eliminates cleavage. We attribute this to a competition of Mg(II) with Fe(II) for binding the EDTA moiety of MPE, rather than to an effect on the MPE–Fe(II) affinity for RNA; similar results have been obtained with DNA (Hertz-

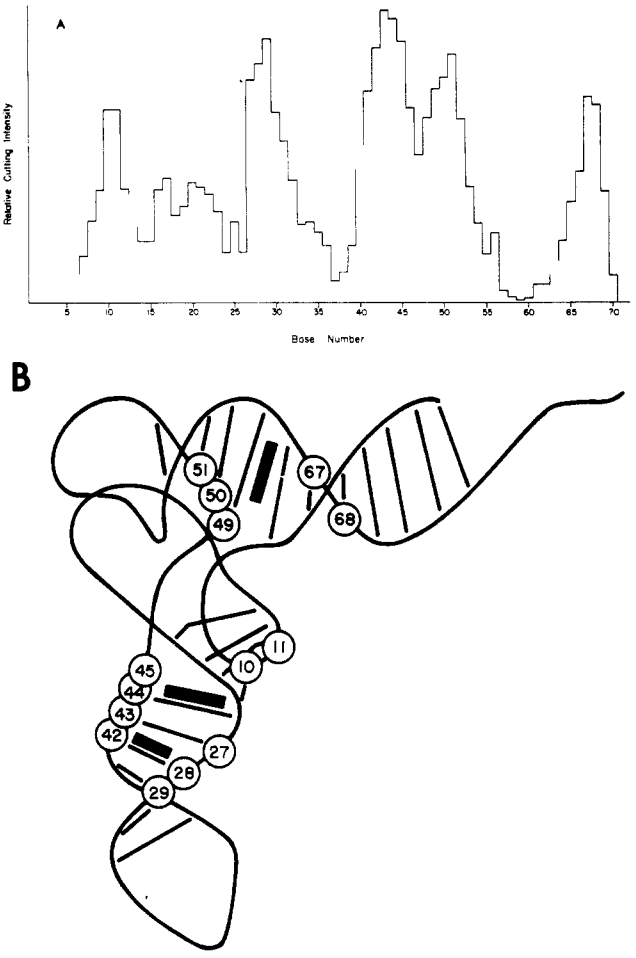

FIGURE 3: (A) Relative intensities of MPE–Fe(II) cleavages in the $tRNA^{Phe}$ sequence. The data were derived from densitometer scans of the gel in Figure 2 and other gels. Poly(A)-poly(U) did not compete for cleavage at positions 13, 40, and 63, so these positions are left blank. (B) Location of the major MPE–Fe(II) cleavage sites in the $tRNA^{Phe}$ crystal structure. Rectangles indicate possible binding locations for the methidium intercalator.

berg & Dervan, 1984). Sufficient cleavage occurs in the presence of 1 mM Mg(II) to obtain a gel pattern, though it may be impractical to estimate equilibrium constants with Mg(II) present.

Cleavage of a 16S rRNA Fragment by MPE–Fe(II). The preceding paper describes the structure of a 345-base fragment of *E. coli* 16S rRNA covering the S8/S15 protein binding domain (Kean & Draper, 1985). The cleavage of this RNA by MPE–Fe(II) is shown in Figure 4. At 2 μM MPE–Fe(II) cuts occur in many regions of the molecule, but at lower concentrations only five sets of cuts persist. These are all clustered in one region of secondary structure, and their positions are shown in Figure 5. Two pairs of these confirm the secondary structure already deduced by structure mapping; i.e., cut sites are staggered on opposite sides of a known helix (positions 662, 673, 735, and 745). There is one set of cuts centered around base 727 which is in a region thought to have a specific structure but with no obvious Watson–Crick pairing possibilities (Kean & Draper, 1985). MPE–Fe(II) cutting in this region could be a consequence of the tertiary folding of the molecule bringing these bases close to one of the helical MPE–Fe(II) sites or a consequence of direct MPE–Fe(II) binding to an unusual tertiary structure. These possibilities are considered further under Discussion.

Affinity of MPE for Specific Sites in tRNA and rRNA Molecules. The affinity of MPE–Fe(II) for individual sites in tRNA or the rRNA fragment was estimated by following the change in cleavage intensity with varying MPE–Fe(II) concentration. We found that much more reproducible free MPE–Fe(II) concentrations were obtained by buffering a fixed total MPE–Fe(II) concentration with increasing concentrations of poly(A)-poly(U), rather than varying the total MPE–Fe(II) concentration.[2] The final results, cleavage intensity as a function of free MPE–Fe(II) concentration, were plotted in the familiar double-reciprocal format to obtain affinity constants (see Figure 6 and Materials and Methods). The results were not affected by the order of MPE–Fe(II), poly(A)-poly(U), and tRNA or rRNA addition. With the tRNA only the acceptor and T helix cutting sites gave reasonable data (affinities of about 10^6 M^{-1}; see Figure 6A); the other sites appeared roughly equivalent to poly(A)-poly(U) in affinity. Cutting sites in the F61 RNA were much stronger and gave rather reproducible affinities from gel to gel; these results are summarized in Table III. Different clusters of cuts that are actually part of the same MPE binding site (e.g., on opposing strands of a helix intercalation site) must obviously show the same apparent binding affinity.

Table III: MPE–Fe(II) Affinities for Individual Sites in F61 RNA[a]

cutting site	MPE–Fe(II) affinity (μM^{-1})
G661	26
G671	20
G727	56
C735	26
A746	12

[a] Binding affinities determined from slopes and intercepts of 1/(peak intensity) vs. 1/(free MPE). Affinities are averages from three separate determinations; the standard errors are about 30%.

We made some attempt to detect cooperative or anticooperative interactions between the different sites on tRNA or F61 RNA by incubating the RNA for long times (60 min) with free MPE–Fe(II) concentrations on the order of 10^{-8} M and comparing these cleavage patterns with patterns obtained at 10^{-7}–10^{-6} M MPE–Fe(II). No differences in relative intensities were found, and we conclude that the MPE–Fe(II) binding sites are approximately independent.

Ethidium Affinity for F61 RNA Sites. The affinities of ethidium and MPE–Fe(II) for sites in the F61 RNA were compared in a competition experiment. As expected, at high concentrations of ethidium MPE–Fe(II) is completely displaced from the RNA and no cutting is observed. The decreases in cutting intensities with increasing ethidium concentration are plotted in Figure 7 for the different F61 RNA sites. Relative affinites of MPE–Fe(II) and ethidium for the individual sites can be extracted from these data by the relation

$$\frac{I}{I_0} = \frac{K_M[M]}{1 + K_M[M] + K_E[E]}$$

where I is the cutting intensity, I_0 is the cutting intensity in

[2] We have noted that the fluorescence of MPE–Fe(II) in the presence of 2 mM DTT decreases significantly over a 20-min period, presumably because the radicals produced by the Fe(II)–DTT system are reacting with the methidium moiety. Excess poly(A)-poly(U) stabilizes the fluorescence, probably because intercalation protects the methidium against reaction. Thus, using poly(A)-poly(U) to buffer the free MPE–Fe(II) concentration probably also stabilizes the compound significantly. The self-degradation of free MPE accounts for the difficulty we had in determining binding constants by direct titrations of a cutting site with low MPE–Fe(II) concentrations. The decrease in free MPE–Fe(II) concentration that occurs in our 20-min incubations does bias our affinity constant measurements, but we estimate that this is no more than a 20% error.

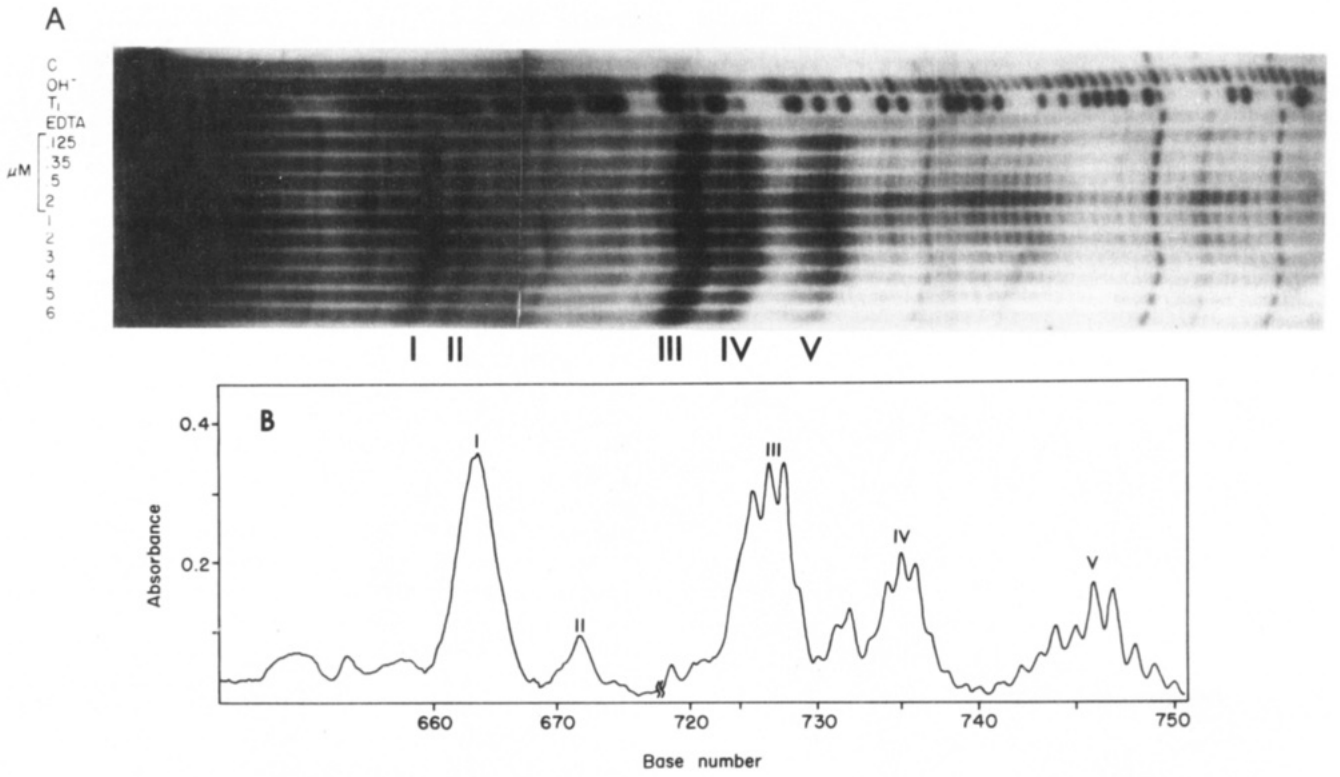

FIGURE 4: (A) Sequencing gel displaying MPE–Fe(II) cutting sites in the F61 RNA fragment. Lanes C, OH^-, and T_1 are as in Figure 2. EDTA indicates 20 μM EDTA–Fe(II) reacted with the RNA under the same conditions as for MPE–Fe(II). 0.125, 0.25, 0.5, and 2 μM indicate reaction with that concentration of MPE–Fe(II) under standard conditions. Lanes marked 1–6 are reactions with 1 μM MPE–Fe(II) and 0, 4.38, 8.75, 17.5, 35, and 70 μM poly(A)-poly(U) base pairs, respectively. (B) Densitometer scan showing relative intensities of the MPE–Fe(II) cutting sites in F61 RNA. Roman numerals correspond to the cutting sites numeraled in (A). Base numbering for peaks I and II is approximate.

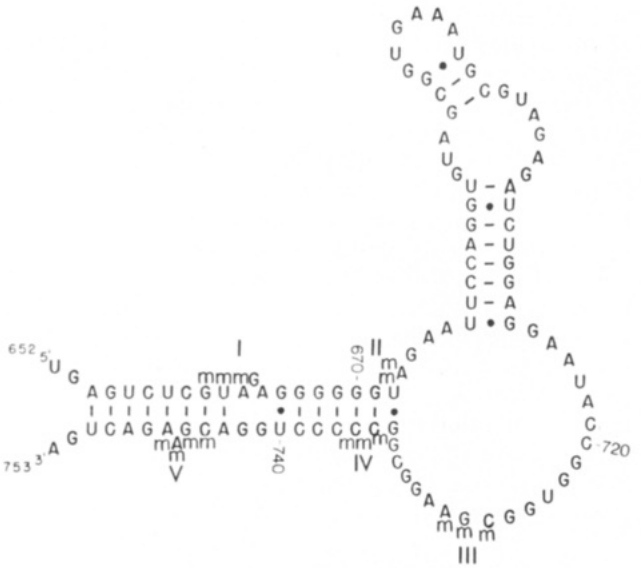

FIGURE 5: Map of MPE–Fe(II) cutting sites in the 16S RNA secondary structure. Secondary structure shown is that proposed by Woese et al. (1983) for bases 652–753 in the 16S ribosomal RNA sequence. Strong cutting by MPE–Fe(II) is indicated by "m"; Roman numerals correspond to Figure 4. Positions of cleavages at sites II–V are taken from Figure 4; site I positions are taken from one gel of 5′-end-labeled RNA which resolved these bases. The cutting locations at 672–673 have never been resolved and could be in error by ±1 base.

the absence of ethidium, K_M and K_E are the site affinities for MPE–Fe(II) and ethidium, and [M] and [E] are the free MPE–Fe(II) and ethidium concentrations, respectively. The competition data show that the ethidium affinity for these RNA sites is 3–5 times weaker than the MPE–Fe(II) affinity; this is in contrast to the results obtained with synthetic poly(A)-poly(U), which binds ethidium with affinity equal to or somewhat greater than MPE–Fe(II). The ratio of the MPE–Fe(II) to ethidium affinities appears roughly the same at all the F61 RNA sites; thus, the absolute ethidium affinities are between 4×10^6 and 2×10^7 M^{-1}.

Discussion

The structural information obtainable from a structure mapping experiment is limited by how well the specificity of the cleavage reagent is understood. Ethidium, closely related to the methidium intercalator moiety of MPE–Fe(II), has been extensively studied in complexes with various synthetic oligo- and polynucleotides and tRNA. To "calibrate" MPE–Fe(II), we have studied its cleavage of yeast $tRNA^{Phe}$, the only RNA with a well understood secondary and tertiary structure. In the following discussion we consider the specificity of the MPE intercalator and the possible structures for the 16S rRNA fragment consistent with the MPE–Fe(II) cleavage sites and affinities.

Influences of Helix Structure on Intercalation. Intercalation of a planar molecule between the base pairs of a DNA or RNA helix requires considerable alteration of the helix conformation. Stacking between consecutive base pairs is disrupted, with accompanying extension of the polynucleotide backbone and unwinding of the helix; this may require a considerable investment of free energy (Breslauer et al., 1975; Gralla & Crothers, 1973). The overall affinity of ethidium or MPE for a particular helix site will reflect both the stability of the disrupted base stacking and the favorable stacking between the phenanthrolinium ring and the bases in the final complex: thus, ethidium (or MPE) affinity for a helix will vary with sequence and structure. Equilibrium studies with synthetic polynucleotides do show considerable dependence of ethidium affinity on sequence (Bresloff & Crothers, 1981; Krugh & Reinhardt, 1975), and the unusual base pair I-A in

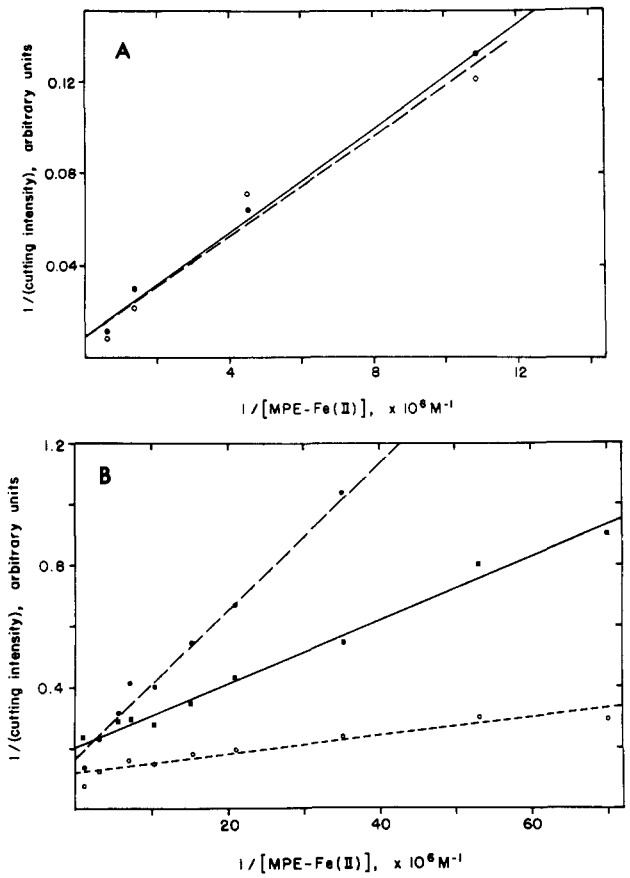

FIGURE 6: Double-reciprocal plots of MPE–Fe(II) titration of individual sites in an RNA. (A) Titration of cutting sites at bases 51 (—) and 67 (---) in $tRNA^{Phe}$; calculated affinity constants are 0.94 and 0.86 μM^{-1}, respectively. (B) Titration of cutting sites at bases 746 (---), 735 (—), and 727 (---) in F61 RNA; calculated affinity constants are 8.5, 20.8, and 41.6 μM^{-1}, respectively.

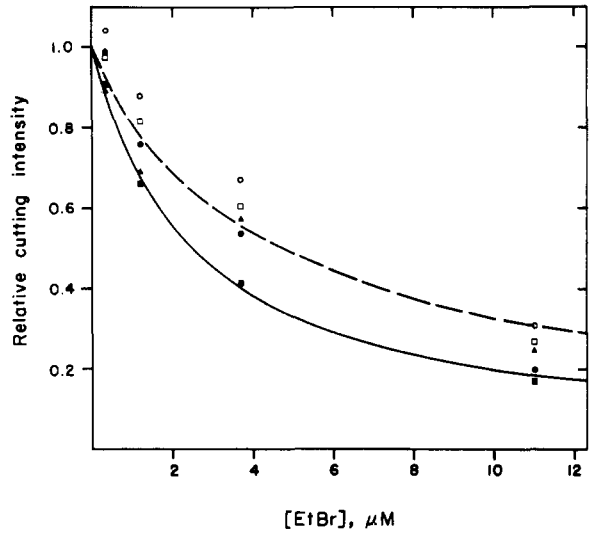

FIGURE 7: Competition of ethidium bromide for MPE–Fe(II) binding sites in F61 RNA. Plotted are the cutting intensities at individual sites at different ethidium concentrations; the MPE–Fe(II) concentration in all reactions was 1 μM. Curves are calculated as described in the text with K_M = 20 μM^{-1} and K_E = 4 (---) or 7 (—) μM^{-1}.

a poly(I)-poly(C) helix enhances ethidium affinity by a factor of about 20 (Helfgott & Kallenbach, 1979). In all these studies there is about a 100-fold variation in ethidium affinity with helix sequence, and the highest affinity of ethidium for a synthetic polymer helix site is about 3×10^6 M^{-1} (at an ionic strength of 0.1 M (NaCl).

Comparison of MPE and Ethidium Binding to RNA. Methidium and ethidium differ by only a methylene group and should have similar intercalation properties. However, the propyl-EDTA moiety of MPE might be expected to enhance the methidium affinity for nucleic acids via hydrophobic interactions of the propyl group in the minor groove or hydrogen bonding of the EDTA to sugars or bases. Such an enhancement is observed with the F61 RNA intercalation sites: the MPE–Fe(II) affinity is 3–5 times higher than the ethidium affinity for the same sites. Burial of a methylene group in a hydrophobic environment can strengthen an interaction by a factor of about 3 (Tanford, 1962), so the observed affinity difference seems reasonable.

A different situation is found when the affinities of MPE–Fe(II) and ethidium for synthetic double helices are compared: ethidium binds as least as well as MPE–Zn(II) to poly(A)-poly(U), and perhaps more strongly. Hertzberg & Dervan (1984) also found that ethidium binds a factor of 8 more strongly than MPE–Ni(II) to DNA. We have considered three possible explanations for why MPE has an apparently low affinity for poly(A)-poly(U):

(i) Hertzberg & Dervan (1984) suggested that MPE–Mg(II) might have a substantially larger component of nonintercalative binding to a helix than ethidium. This was advanced as an explanation for the low unwinding angle measured for MPE–Mg(II) with DNA (11° vs. 26° for ethidium). If such binding occurred but was not detected in our fluorescence measurements, it would tend to make our affinity measurements for intercalation appear low.

(ii) Anticooperativity between MPE–Zn(II) molecules bound to poly(A)-poly(U) may have biased our measurements to give very low apparent affinities; anticooperativity would of course not influence the binding to individual sites in the RNA fragment.

(iii) The propyl-EDTA arm of MPE may interfere with MPE–Zn(II) intercalation in a long double helix, but not influence its binding to particular RNA sites with irregular structure.

The first possibility is unlikely. A large proportion of nonintercalative binding would make the MPE–Zn(II) site sizes much larger than those for ethidium, but our titrations give about three base pairs per bound intercalator for each. Competition with poly(A) (Table II) also shows that nonintercalative binding must be at least 2 orders of magnitude weaker than intercalative.

The second possibility, anticooperativity, is certainly plausible. The 1– charge of the EDTA–Fe(II) complex could contribute some repulsion between MPE–Fe(II) molecules closely bound on a long polymer; a reduction in affinity of a factor of 3 for intercalators bound 7 Å apart is possible. The interplay between site size, cooperativity (or anticooperativity), and intrinsic binding affinity is very difficult to sort out for ligands binding long polymers (McGhee & von Hippel, 1974), and our estimates of intrinsic affinities could be off by factors of 2 or 3.

The last possibility should also be taken seriously. Extensive studies with derivatives of the phenanthrolinium ring of ethidium (Gabbay et al., 1973a,b) and other intercalators (Adawadkar et al., 1975; Kapicak & Gabbay, 1975) have shown that fairly minor modifications of an intercalator can markedly alter the distortion it introduces into a helix and its affinity for different polymers. Especially relevant is the observation that shortening a tether linking a charged group with an intercalator changes binding from full intercalation to only partial insertion into a helix (Kapicak & Gabbay,

1975). Our salt dependence data (Table I) imply that the EDTA–metal ion complex, with a 1– charge, remains outside of the dense counterion atmosphere surrounding the RNA; this could restrain the methidium from full intercalation into a helix, weakening binding and altering the unwinding angle. Helices of unusual or irregular structure, as found in tRNA or rRNA, may not impose the same constraints on the intercalator and obtain a higher free energy of interaction with MPE.

It is most likely that the different relative MPE and ethidium affinities found with different RNAs are the result of both the difficulty of measuring intrinsic affinity constants with synthetic polymers and small differences in the way ethidium and MPE are able to interact with different RNAs. Whether or not MPE and ethidium bind RNA by slightly different mechanisms, the conclusion that ethidium binds sites in the RNA fragment with an unusually high affinity of $\approx 10^7$ M^{-1} remains.

MPE–Fe(II) Binding Sites in tRNA. The cleavage pattern obtained with MPE–Fe(II) and $tRNA^{Phe}$ implies the existence of several MPE–Fe(II) binding sites. All of the strong cutting sites can be interpreted in terms of MPE–Fe(II) binding at helix intercalation sites. The cutting in the anticodon stem is as expected for a single MPE intercalation site: there are two cutting sites on opposite sides of the helix, and cutting is most intense on the 3′ sides of the binding site. The cuts obtained in the acceptor and T loops are unusual in that only one of the two strands is cut in each helix. One possible explanation is that some distortion in the helix may allow the EDTA–Fe(II) complex access to only one side of the groove. The sharp bend in the backbone between bases 7 and 8, for instance, would probably reduce the cutting intensity at bases 8 and 9 if MPE–Fe(II) were intercalated at the base of the acceptor helix. However, there is no obvious reason why intercalation in the T helix should give cutting in only one strand. The more likely possibility is that the two sets of cuts derive from the same binding site, since the two helices actually form a single, longer coaxial helix (Holbrook et al., 1978). The intercalation site would then be located at the junction between the two helices, i.e., between pairs U7-A66 and C49-G65.

The cuts at bases 10–13 suggest another MPE–Fe(II) binding site located in the D stem on either side of the m^2G10-C25 pair. The complementary strand cuts should then be in the vicinity of bases 25–29. This section partially overlaps with cutting from the anticodon stem site, and the cutting intensity at G26 is difficult to assess, so it is difficult to determine which side of m^2G-C25 is the binding site. One side would again place a binding site between two coaxial helices (the D and anticodon).

Conditions that favor formation of $tRNA^{Phe}$ tertiary structure limit the binding of ethidium bromide to a single binding site with an affinity of about 5×10^6 M^{-1} (Urbanke et al., 1973; Tao et al., 1970). There has been some controversy about the location of this site. Studies by Liebman et al. (1977) indicated that ethidium bromide diffused into a $tRNA^{Phe}$ crystal is located at a single nonhelical site, partially stacked on the U8-A14 tertiary pair. This observation was interpreted to mean that ethidium may bind to structured RNA molecules strongly by nonintercalative modes. NMR and fluorescence energy-transfer measurements favored a site at the base of the acceptor helix (Jones et al., 1978; Wells & Cantor, 1977). We find no cutting that would suggest MPE binding in the tertiary structure near U8 and think it unlikely that the site observed by Liebman et al. reflects strong binding in solution. The apparent intercalation of MPE–Fe(II) between the acceptor and T helices is reasonably consistent with the NMR and fluorescence studies. Although Mg^{2+} may have some specific effects on $tRNA^{Phe}$ tertiary structure (Draper, 1985), we did not find any effect of 1 mM Mg^{2+} on the cutting pattern.

MPE Binding Sites in a 16S rRNA Fragment. Although the 345-base fragment of 16S rRNA we have examined has 11 helices (Kean & Draper, 1985), only five sets of cuts are observed with MPE–Fe(II) at low concentrations, and these are clustered in one region of the molecule.

Two of the strong cutting sites (around A746 and C661) are readily interpreted as representing a helix intercalation site near a single base bulge, A746. It at first seemed likely to us that intercalation should occur at the position of the bulge, since the bulge might reduce the energy required to stretch the helix backbone and thus enhance intercalator affinity. However, the positions of the strongest cuts are more consistent with intercalation at the *adjacent* site (between base pairs C659-G745 and G660-C744). J. Nelson and I. Tinoco have compared ethidium binding to synthetic DNA oligomers differing by a single bulged C and find that their results are most consistent with 10-fold enhanced intercalation on either side of the bulge (personal communication). These results are certainly consistent with both the position and the affinity of the intercalation we observe. Pyrimidine–purine sequences have a particularly high affinity for ethidium (Krugh & Reinhardt, 1975), which may explain why MPE–Fe(II) intercalates strongly at the C-G sequence and not at the other side of the A746 bulge. It is of course possible that other aspects of the RNA structure such as potential interactions of A746 with other parts of the molecule may influence the structure of this helix and its affinity for intercalators.

Another pair of cutting sites suggests intercalation at or near the end of a helix (near pair G671-C735). The cuts around G670 are very faint, which may indicate that the EDTA–Fe(II) complex is constrained near the 3′ side of the helix end. It is not apparent from the RNA secondary structure in this region why this site should have a particularly high affinity for intercalators.

The fifth set of cuts, between 723 and 728, is not readily identified with any helical structure. No stable Watson–Crick helices are predicted within this bulge loop; we also find that MPE–Fe(II) cutting is unchanged in a smaller RNA fragment covering bases 648–759, ruling out the possibility of long-range pairing (J. Vartikar and D. E. Draper, unpublished observations). However, G727 is in an unusual conformation: residues on either side are strongly cut by T_2 RNase, an enzyme specific for unstacked, unpaired residues, while G727 itself is recognized by the helix-specific V_1 nuclease (Draper & Kean, 1985). V_1 nuclease activity requires four or five bases stacked in a roughly helical conformation (H. Lowman and D. E. Draper, unpublished observations), so it is difficult to understand how a V_1-sensitive nucleotide can be flanked by unstacked residues. A possibility is that the RNA tertiary folding stacks G727 with some other helical region of the molecule so that V_1 recognizes it as part of a helix. If it were interacting with bases near the second MPE–Fe(II) intercalation site (i.e., near G671-C735), then a single MPE–Fe(II) intercalation might result in three sets of backbone cleavages (U672, G727, and C736).

Another possible explanation for the MPE–Fe(II) cleavages around G727 is that the RNA tertiary structure forms a high-affinity intercalation site without a regular Watson–Crick helix. The binding affinities we calculate for the separate cutting sites do show a slightly higher affinity at the G727 site, suggesting it is a separate binding site. However, the affinity

difference is only slightly larger than the standard errors and may not be significant.

Utility of MPE–Fe(II) as a Structure Mapping Reagent. The fact that MPE–Fe(II) gives a "spray" of cuts around a specific site limits its utility as a structure mapping reagent. The majority of nucleotides in tRNA, for instance, show significant cleavage, and it would probably be difficult to deduce the cloverleaf base pairing scheme from this information alone. However, in a larger RNA with only a few strong intercalation sites, the sets of strong cuts may be aligned to give useful information about the folding of the RNA chain. Similar findings have been made by N. Kyle Tanner and T. Cech, who have examined the reaction of tRNA and an intervening sequence RNA with MPE–Fe(II) (personal communication): the larger intervening sequence gives relatively few sets of cuts, but the sparsity of the cutting allows deductions about the RNA folding to be made.

Possible Functions of High-Affinity Intercalator Sites in RNA. An unusual feature of all the MPE–Fe(II) cutting sites is their high afinity for both MPE–Fe(II) and for ethidium. The ethidium affinity of 10^7 M^{-1} at 37 °C in 0.1 M NaCl is severalfold stronger than measured for any synthetic polymer or tRNA, which indicates that the binding site structures are not a regular A-form RNA helix. The clustering of these unusual binding sites in one region of the RNA fragment suggests that they may be of functional significance; we can imagine two possibilities. First, the site may be important for protein–RNA interactions. A number of model studies have shown that tyrosine and tryptophan residues are capable of intercalation between polynucleotide bases (Hélène et al., 1975; Gabbay et al., 1973a,b) and this mechanism is probably important for fd gene V protein (Anderson et al., 1975; O'Connor & Coleman, 1983; Brayer & McPherson, 1984) and T4 phage gene 32 protein (Anderson & Coleman, 1975; Prigodich et al., 1984) binding to single-stranded DNA. An RNA molecule could conceivably promote a site-specific interaction with a particular protein by creating, via appropriate secondary and tertiary structures, a site designed to accept an aromatic protein residue. A mechanism of this sort may take place with ribosomal protein L4: tyrosine-35 in this protein is readily cross-linked by UV irradiation to U615 in the 23S rRNA sequence (Maly et al., 1980). U615 is probably located in an exposed hairpin loop (Noller et al., 1981); the MPE–Fe(II) cutting site at G727 is also flanked by single-stranded residues. Ribosomal protein S15 contains two tyrosines and two phenylalanines (Morinaga et al., 1976) and probably interacts with the helices at 655–672/734–751 (Müller et al., 1979; Zimmermann & Singh-Bergmann, 1979); it therefore is in a position to take advantage of the intercalaction sites.

The other possible function of the high-affinity intercalator sites is maintenance of specific RNA–RNA interactions; i.e., the site could be designed to bind a base residue from another region of the rRNA or a substrate RNA. For example, the 5′ base of the tRNA anticodon in the ribosomal P site is known to stack with base C1400 in the 16S rRNA (Prince et al., 1982; Ofengand et al., 1982). The RNA structure in the vicinity of C1400 bears some resemblance to the G727 MPE–Fe(II) cutting site: there is no obvious secondary structure between bases 1392 and 1408, and bases on the 3′ side of C1400 are readily accessible to single strand specific reagents though C1400 itself is not (Douthwaite et al., 1983). RNA–RNA stacking interactions at the strong MPE binding sites could stabilize tertiary interactions in the 16S rRNA or help orient tRNA or mRNA molecules on the surface of the ribosome.

Registry No. MPE–Fe(II), 80105-72-2; DDT, 3483-12-3; poly(A)-poly(U), 24936-38-7; EthBr, 1239-45-8; MPE–Zn(II), 80105-74-4; Na, 7440-23-5; Mg, 7439-95-4.

REFERENCES

Adwadakar, P., Wilson, W. D., Brey, W., & Gabbay, E. J. (1973) *J. Am. Chem. Soc. 95*, 1959–1961.

Anderson, R., & Coleman, J. E. (1975) *Biochemistry 14*, 5485–5491.

Anderson, R., Nakashima, Y., & Coleman, J. E. (1975) *Biochemistry 14*, 907–917.

Brayer, G. D., & McPherson, A. (1984) *Biochemistry 23*, 340–349.

Breslauer, K. J., Sturtevant, J. M., & Tinoco, I. (1975) *J. Mol. Biol. 99*, 549–565.

Bresloff, J. L., & Crothers, D. M. (1981) *Biochemistry 20*, 3547–3553.

Britten, R. (1962) *C. R. Trav. Lab. Carlsberg 32*, 371–380.

Brown, R. S., Hingerty, B. E., Dewan, J. C., & Klug, A. (1983) *Nature (London) 303*, 543–546.

D'Alessio, J. M. (1982) in *Gel Electrophoresis of Nucleic Acids* (Rickwood, D., & Hames, B. D., Eds.) pp 173–197, IRL Press, Oxford.

Douthewaite, S., Christensen, A., Garrett, R. A. (1983) *J. Mol. Biol. 169*, 249–279.

Draper, D. E. (1985) *Biophys. Chem. 21*, 91–101.

Gabbay, E. J., Scofield, R. E., & Baxter, C. S. (1973a) *J. Am. Chem. Soc. 95*, 7850–7857.

Gabbay, E. J., Sanford, K., Baxter, C. S., & Kapicak, L. (1973b) *Biochemistry 12*, 4021–4029.

Garrett, R. A., & Oleson, S. O. (1982) *Biochemistry 21*, 4823–4830.

Gralla, J., & Crothers, D. M. (1973) *J. Mol. Biol. 73*, 497–511.

Hélène, C., Dimicoli, J.-L., & Brun, F. (1971) *Biochemistry 21*, 3802–3809.

Helfgott, D. C., & Kallenbach, N. R. (1979) *Nucleic Acids Res. 7*, 1011–1017.

Hertzberg, R. P., & Dervan, P. B. (1982) *J. Am Chem. Soc. 104*, 313–315.

Hertzberg, R. P., & Dervan, P. B. (1984) *Biochemistry 23*, 3934–3945.

Holbrook, S. R., Sussman, J. L., Warrant, R. W., & Kim, S.-H. (1978) *J. Mol. Biol. 123*, 631–660.

Jones, C. R., Bolton, P. H., & Kearns, D. R. (1978) *Biochemistry 17*, 601–607.

Kapicak, L., & Gabbay, E. J. (1975) *J. Am. Chem. Soc. 97*, 403–408.

Kean, J. M., and Draper, D. E. (1985) *Biochemistry* (preceding paper in this issue).

Krugh, T. R., & Reinhardt, C. G. (1975) *J. Mol Biol. 97*, 133–162.

Laskey, R. A. (1982) *Methods Enzymol. 65*, 363–371.

LePecq, J.-B., & Paoletti, C. (1967) *J. Mol. Biol. 27*, 87–106.

Liebman, M., Rubin, J., & Sundaralingam, M. (1977) *Proc. Natl. Acad. Sci. U.S.A. 74*, 4821–4825.

Maly, P., Rinke, J., Ulmer, E., Zwieb, C., & Brimacombe, R. (1980) *Biochemistry 19*, 4179–4188.

McGhee, J. D., & von Hippel, P. H. (1974) *J. Mol. Biol. 86*, 469–489.

Morinaga, T., Funatsu, G., Funatsu, G., & Wittmann, H. G. (1976) *FEBS Lett. 64*, 307–309.

Müller, R., Garrett, R. A., & Noller, H. F. (1979) *J. Biol. Chem. 254*, 3873–3878.

Noller, H. F., & Woese, C. R. (1981) *Science (Washington, D.C.) 212*, 403–411.

Noller, H. F., Kop, J., Wheaton, V., Brosius, J., Gutell, R. R., Kopylov, A. M., Dohme, F., Herr, W., Stahl, D. A., Gupta, R., & Woese, C. R. (1981) *Nucleic Acids Res. 9*, 6167–6189.
Ofengand, J., Gornicki, P., Chakraburtty, K., & Nurse, K. (1982) *Proc. Natl. Acad. Sci. U.S.A. 79*, 2817–2821.
Peattie, D., & Gilbert, W. (1980) *Proc. Natl. Acad. Sci. U.S.A. 77*, 4679–4682.
Prigodich, R. V., Casas-Finet, J., Williams, K. R., Konigsberg, W., & Coleman, J. E. (1984) *Biochemistry 23*, 522–529.
Prince, J. B., Taylor, B. H., Thurlow, D. L., Ofengand, J., & Zimmermann, R. A. (1982) *Proc. Natl. Acad. Sci. U.S.A. 79*, 5450–5454.
Record, M. T. R., Lohman, T. M., & deHaseth, P. (1976) *J. Mol. Biol. 107*, 145–158.
Schultz, P. G., & Dervan, P. B. (1983) *Proc. Natl. Acad. Sci. U.S.A. 80*, 6834–6837.
Schultz, P. G., Taylor, J. S., & Dervan, P. B. (1982) *J. Am. Chem. Soc. 104*, 6861–6863.
Tanford, C. (1962) *J. Am. Chem. Soc. 84*, 4240–4247.
Tao, T., Nelson, J. H., & Cantor, C. R. (1970) *Biochemistry 9*, 3514–3523.
Tinoco, I., Martin, F. H., Nelson, J. W., & Pardi, A. (1981) *Macromol. Chem. Phys. Suppl. 4*, 143–153.
Urbanke, C., Römer, R., & Maas, G. (1973) *Eur. J. Biochem. 33*, 511–516.
Wells, B. D., & Cantor, C. R. (1977) *Nucleic Acids Res. 4*, 1667–1679.
Woese, C. R., Gutell R., Gupta, R., & Noller, H. (1983) *Microbiol. Rev. 47*, 621–669.
Wurst, R. M., Vournakis, J. N., & Maxam, A. M. (1978) *Biochemistry 17*, 4493–4499.
Zimmermann, R. A., & Singh-Bergmann, K. (1979) *Biochim. Biophys. Acta 563*, 422–431.

Isolation and Characterization of Z-DNA Binding Proteins from Wheat Germ†

Eileen M. Lafer,* Rui Sousa, Barry Rosen, Anna Hsu, and Alexander Rich

Department of Biology, Massachusetts Institute of Technology, Cambridge, Massachusetts 02139

Received January 10, 1985

ABSTRACT: The preparation of a heterogeneous non-histone protein extract from wheat germ utilizing Br–poly(dG-dC)·poly(dG-dC) (Z-DNA) affinity chromatography is described. The binding characteristics of antibodies against Z-DNA are used as a model system to define important criteria that the DNA binding behavior of a Z-DNA binding protein should display. We show that the wheat germ extract contains DNA binding proteins specific for left-handed Z-DNA by these criteria. The affinity of the proteins measured by competition experiments was approximately 10^5 greater for Br–poly(dG-dC)·poly(dG-dC) (Z-DNA) than for poly(dG-dC)·poly(dG-dC) (B-DNA). The affinity of the proteins for plasmid DNA increases with increasing negative superhelicity which is known to stabilize Z-DNA. The proteins are shown to compete with Z-DNA antibodies for binding to supercoiled plasmids. Finally, the affinity for two plasmids at a given superhelical density is greater for the plasmid containing an insert known to form Z-DNA than for a plasmid without the insert. The proteins exhibit a 2–3-fold greater affinity for stretches of $(dC\text{-}dA)_n\cdot(dT\text{-}dG)_n$ over stretches of $(dG\text{-}dC)_n\cdot(dG\text{-}dC)_n$ when both sequences are induced to form Z-DNA by supercoiling.

Right-handed B-DNA and left-handed Z-DNA [reviewed in Rich et al. (1984)] are two equilibrium structures of double-stranded DNA. Z-DNA is the higher energy form, but it can be stabilized at physiological ionic strengths in a closed circular molecule by negative supercoiling (Singleton et al., 1982; Peck et al., 1982; Nordheim et al., 1982b; Haniford & Pulleyblank, 1983a,b) or by antibody binding (Lafer et al., 1985). Linear polymers can be stabilized as Z-DNA by chemical modifications such as bromination (Moller et al., 1984) or methylation (Behe & Felsenfeld, 1981). Early work on Z-DNA implied a strict requirement for alternating purine–pyrimidine sequences (Wang et al., 1979), but recently nonalternating sequences have been shown in X-ray crystallographic and solution studies to be capable of forming Z-DNA (Wang et al., 1985; Feigon et al., 1985). To assist in the elucidation of the biological role(s) of Z-DNA, we have isolated and characterized naturally occurring Z-DNA specific binding proteins from wheat germ. Wheat germ is a useful tissue to use for protein purification because it is both readily available and low in protease activity. Much work has been done defining the interactions between sequence-specific B-DNA binding proteins and their substrates [reviewed in Pabo & Sauer (1984)]. These studies have only limited usefulness as model systems for Z-DNA binding proteins. Unlike a specific sequence contained within a much longer B-DNA sequence, Z-DNA is a dynamic feature of the double-stranded DNA molecule which can be affected by superhelicity, ionic strength, and protein binding. An example of specific Z-DNA binding proteins is found in antibodies that we have prepared with both low and high affinities (Lafer et al., 1981, 1983, 1985). We consider these antibodies as a model system for naturally occurring Z-DNA binding activity.

By using the binding characteristics of the Z-DNA antibodies, we can define the DNA binding behavior that a Z-DNA binding protein should display. Bromination of poly(dG-dC)·poly(dG-dC) in high salt stabilizes Z-DNA, so a

† This research was supported by the American Cancer Society, the National Science Foundation, and the National Institutes of Health. E.M.L. was supported by a Helen Hay Whitney Foundation fellowship.

0006-2960/85/0424-5070$01.50/0